Atomic resolution (0.97 Å) structure of the triple mutant (K53,56,121M) of bovine pancreatic phospholipase A_2

K. Sekar,[a,b]* V. Rajakannan,[c] D. Gayathri,[c] D. Velmurugan,[c] M.-J. Poi,[d,e] M. Dauter,[f] Z. Dauter[g] and M.-D. Tsai[d,e]

[a]Bioinformatics Centre, Indian Institute of Science, Bangalore 560 012, India, [b]Supercomputer Education and Research Centre, Indian Institute of Science, Bangalore 560 012, India, [c]Department of Crystallography and Biophysics, University of Madras, Guindy Campus, Chennai 600 025, India, [d]Department of Chemistry and Biochemistry and The Ohio State Biotechnology Program, The Ohio State University, Columbus, OH 43210, USA, [e]Academia Sinica, Taiwan, [f]SAIC-Frederick Inc., Basic Research Program, Brookhaven National Laboratory, Building 725A-X9, Upton, NY 11973, USA, and [g]Synchrotron Radiation Research Section, Macromolecular Crystallography Laboratory, NCI and Brookhaven National Laboratory, Building 725A-X9, Upton, NY 11973, USA

Correspondence e-mail: sekar@physics.iisc.ernet.in

PDB Reference: K53,56,121M bovine pancreatic PLA_2, 1vl9, r1vl9sf.

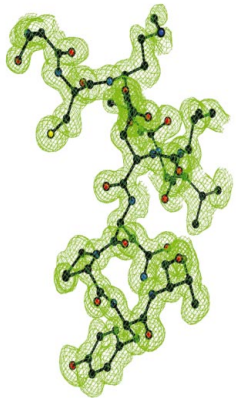

The enzyme phospholipase A_2 catalyzes the hydrolysis of the *sn*-2 acyl chain of phospholipids, forming fatty acids and lysophospholipids. The crystal structure of a triple mutant (K53,56,121M) of bovine pancreatic phospholipase A_2 in which the lysine residues at positions 53, 56 and 121 are replaced recombinantly by methionines has been determined at atomic resolution (0.97 Å). The crystal is monoclinic (space group *P*2), with unit-cell parameters a = 36.934, b = 23.863, c = 65.931 Å, β = 101.47°. The structure was solved by molecular replacement and has been refined to a final R factor of 10.6% ($R_{\rm free}$ = 13.4%) using 63 926 unique reflections. The final protein model consists of 123 amino-acid residues, two calcium ions, one chloride ion, 243 water molecules and six 2-methyl-2,4-pentanediol molecules. The surface-loop residues 60–70 are ordered and have clear electron density.

1. Introduction

Pancreatic phospholipase A_2 (PLA_2), a subfamily of the growing PLA_2 superfamily (Dennis, 1994, 1997), hydrolyzes the *sn*-2 ester bond of 3-*sn*-phospholipids. These calcium-dependent and highly homologous enzymes are typically small (13–15 kDa), but possess several interesting structural features. The PLA_2 enzyme is one of the better characterized lipolytic enzymes, particularly with respect to enzymatic mechanism. The first detailed structural analysis of this enzyme was carried out by Dijkstra and coworkers (Dijkstra *et al.*, 1978, 1981), which together with further biochemical data led to a proposed catalytic mechanism (Scott *et al.*, 1990; Thunnissen *et al.*, 1990; Verheij *et al.*, 1980). In most of the structures of recombinant bovine pancreatic PLA_2 and its mutants, the residues in a surface loop in the region 60–70 have been found to be disordered (Huang *et al.*, 1996; Sekar, Yu *et al.*, 1997; Sekar, Kumar *et al.*, 1998; Sekar, Sekharudu *et al.*, 1998; Sekar *et al.*, 1999, 2003; Yu *et al.*, 2000). The loop has also been found in a well ordered conformation in several structures (Rajakannan *et al.*, 2002; Sekar, Eswaramoorthy *et al.*, 1997; Sekar *et al.*, 2003; Sekar & Sundaralingam, 1999; Steiner *et al.*, 2001). Since mutations of lysine residues to methionine at positions 53, 56, 120 and 121 are found to enhance the binding of the enzyme in zwitterionic interfaces (Yu *et al.*, 2000), three different combinations of these mutations, K53,56M (designated to indicate that lysines at positions 53 and 56 are replaced by methionine residues; Yu *et al.*, 2000), K56,120,121M (similarly mutated at residues 56, 120 and 121; Rajakannan *et al.*, 2002) and K53,56,120M (Sekar *et al.*, 2003, 2004), have been crystallized and studied. To further unravel the structural features associated with these mutations, we have undertaken the crystal structure of the triple mutant K53,56,121M of bovine pancreatic PLA_2.

2. Materials and methods

2.1. Construction of K53/56/121M PLA_2 mutant

The mutant PLA_2 was generated by site-directed mutagenesis. The following complementary sets of oligonucleotides were used: 5′-CATGATAATTGCTATATGCAAGCTAAAAAACTT-3′ (K53M), 5′-TGCTATAAACAAGCTATGAAACTTGATAGCTGC-3′ (K56M) and 5′-CAAGAATCTTGATAAAATGAACTGTTAAGCTTCT-3′

(K121M). The Quickchange method by Stratagene was employed using pET25b(m)-proPLA2 as template. The single mutant K53M was first generated and the double (K53,56M) and triple (K53,56,121M) mutants were then generated using the single mutant and double mutant, respectively, as template DNA. The recombinant bovine pancreatic PLA_2 protein was expressed in *Escherichia coli* BL21(DE3) pLysS strain as inclusion bodies and was refolded and purified as described elsewhere (Liu *et al.*, 1995; Zhu *et al.*, 1995).

2.2. Crystallization, data collection and processing

The protein samples were lyophilized upon dialysis against distilled H_2O following a QSFF ion-exchange chromatographic separation. The QSFF buffer consisted of 10 m*M* Tris adjusted to pH 8.4–8.5 using NaOH and the elution gradient used was 50–100 m*M* NaCl. The elution fraction collected was between 50 and 100 ml in volume and was then dialyzed against 8 l of distilled H_2O. The usual range of final protein product was between 15 and 30 mg. Therefore, the estimated salt components carried over were between 10 and 125 m*M* NaCl and 5 and 15 m*M* Tris. The exact salt content carried over from the purification process was difficult to determine because the purification process could vary slightly from batch to batch owing to the elaborate procedures involved.

Lyophilized protein (powder form) samples of the present triple mutant were dissolved in 50 m*M* Tris buffer pH 7.2 containing 5 m*M* $CaCl_2$ to a final protein concentration of 17–20 mg ml^{-1}. The crystallization droplet contained 5 µl protein solution and 3 µl 60%(*v*/*v*) 2-methyl-2,4-pentanediol (MPD) and the reservoir contained 70%(*v*/*v*) MPD. The hanging-drop vapour-diffusion method was employed and crystals appeared in about two weeks. High-quality X-ray diffraction data were collected from a single crystal measuring 0.40 × 0.30 × 0.30 mm at liquid-nitrogen temperature (100 K). The intensity data were collected on beamline X9B (National Synchrotron Light Source, Brookhaven National Laboratory, Upton, NY, USA) using an ADSC Quantum 4 CCD detector. Data were processed and scaled using the *HKL*2000 suite of programs (Otwinowski & Minor, 1997) and the associated statistics are given in Table 1.

Table 1
Crystal and geometrical parameters of the triple mutant K53,56,121M of bovine pancreatic PLA_2.

Values in parentheses are for the highest resolution shell.

Data-collection details	
Wavelength (Å)	0.979
Unit-cell parameters (Å, °)	a = 36.934, b = 23.863, c = 65.931, β = 101.47
Space group	*P*2
Resolution range (Å)	20.0–0.97 (1.00–0.97)
No. observations	627336 (44605)
No. unique reflections	67307 (6666)
Completeness of data	100.0 (100.0)
R_{merge}	0.051 (0.486)
$I/\sigma(I)$	39.3 (3.5)
Redundancy	9.3 (6.7)
Model details	
Protein atoms	954
Calcium ions	2
Chloride ions	1
MPD atoms	48
Water O atoms	243
Refinement details	
No. reflections used in refinement	63926
No. parameters in the final run of *SHELXL*	12676
R factor for $F > 4\sigma$ (%)	10.6
R_{free}	13.4
R factor for all data (%)	11.7
Goodness of fit	2.4
Mean isotropic equivalent B factor (Å^2)	20.5

2.3. Structure solution and refinement

The 1.9 Å resolution model of bovine pancreatic PLA_2 (Rajakannan *et al.*, 2002; PDB code 1gh4) was used for molecular replacement (Navaza, 1994). The resultant model was subjected to rigid-body refinement, which led to an R factor of 23.5% [R_{free} = 24.1%; Brünger, 1992). At this stage, 20 cycles of restrained refinement with *REFMAC* (Murshudov *et al.*, 1999) were performed and the resolution was extended stepwise to 0.97 Å. Subsequently, ten cycles of refinement using *REFMAC* combined with *ARP*/*wARP* (Perrakis *et al.*, 1999) were performed and a total of 164 water molecules were located and added to the model, giving an R factor ($F > 4\sigma$) of 19.5% (R_{free} = 21.3%). Inspection of the difference electron-density maps indicated minor adjustments for the side chains of Trp3, Gln4, Leu31 and Lys120 and these were performed with the molecular-modelling program *FRODO* (Jones, 1985). Moreover, clear signs of anisotropy present in the electron density for several residues suggested possible alternate side-chain conformations. 20 cycles of anisotropic refinement were carried out for all the residues with inclusion of H atoms at calculated positions and decreased the R factor to 14.3% (R_{free} = 17.6%). A manual rebuilding step was performed followed by a few cycles of conjugate-gradient least-squares refinement using *SHELXL* (Sheldrick & Schneider, 1997). The side chains of 14 amino-acid residues (Leu2, Trp3, Gln4, Lys10, Leu31, Met53, Met56, Lys108, Lys113, Lys116, Leu118, Lys120, Met121 and Asn122) were modelled with more than one side-chain position. Modelling of alternate conformations was carried

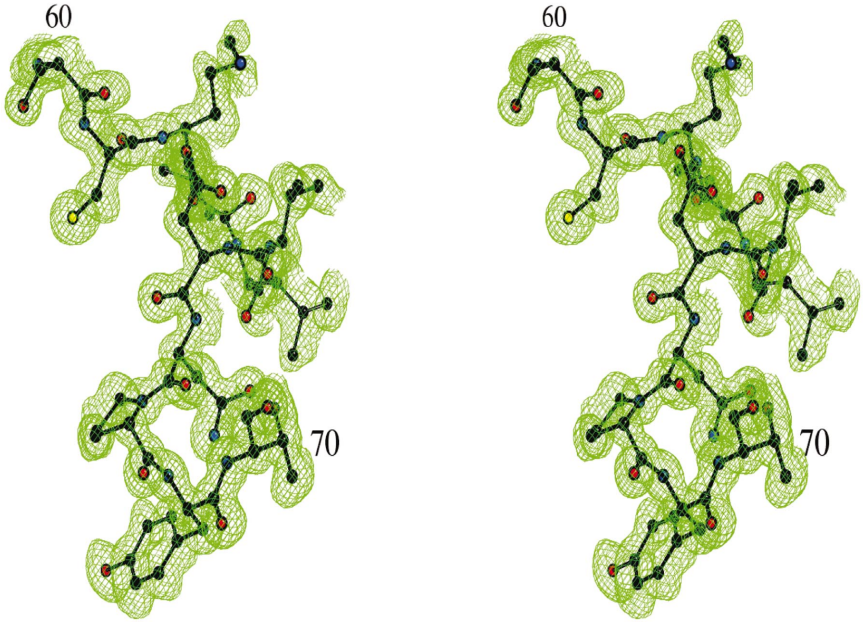

Figure 1
A stereoview of the difference electron-density ($2|F_o| - |F_c|$) map showing the ordered surface loop and the map contoured at the 1.2σ level.

out in the anisotropic model. A total of six MPD molecules, two calcium ions and one chloride ion were identified and included in the refinement. The positions of the second calcium ion and the chloride ion are consistent with those found in the prior atomic resolution structure of the enzyme (Steiner *et al.*, 2001) and also with our recent structure of the K53,56,120M mutant (Sekar *et al.*, 2004). Refinement of the extensively rebuilt model, which included 11 further residues (Arg43, Asn50, Gln54, Lys57, Leu58, Lys62, Ser74, Ser76, Glu81, Ser86 and Glu114) with alternate conformations, led to an *R* factor of 12.1% (R_{free} = 14.9%). Additional water O atoms were located and included in the refinement (water molecules with occupancies lower than 0.2 are removed from the refinement), which reduced the final *R* factor to 10.6% (R_{free} = 13.4%) and those that had higher than 0.95 were treated as having unit occupancy. These water molecules were also refined anisotropically. The *R* factor at this stage was 11.7% for all reflections. Refinement statistics are given in Table 1.

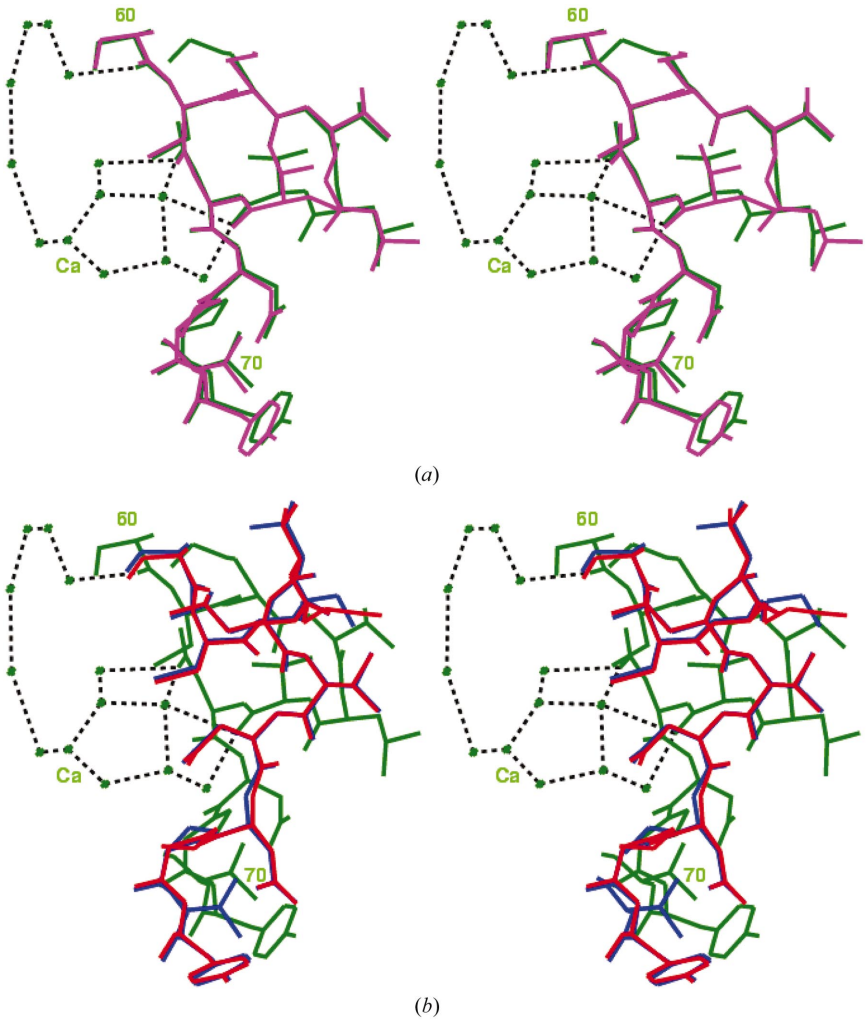

Figure 2
(*a*) A stereoview of the hydrogen-bonding network (dashed lines) between the second calcium ion (Ca) and the surface-loop residues of the present model (green) along with the superposition of the corresponding region of the triple mutant (K56,120,121M) (magenta) is shown. (*b*) A stereoview showing the superposition of the surface-loop residues observed in the atomic resolution structure of the wild type (red) and the orthorhombic form of the recombinant PLA_2 (blue) with the present model (green) is shown. The hydrogen-bonding network (dashed lines) involving the second calcium ion (Ca) and the surface-loop residues of the refined model is also represented.

3. Results and discussion

3.1. Quality of the model

The final refined model consists of 123 amino-acid residues, two calcium ions, one chloride ion, six MPD molecules and 243 crystallographic water molecules (137 water molecules have unit occupancy). The conventional *R* factor ($F > 4\sigma$) for the refined model is 10.6% (R_{free} = 13.4%). In general, the electron density is clear for all the residues. A Ramachandran plot calculated using *PROCHECK* (Laskowski *et al.*, 1993) shows 92.7% of the residues in most favoured regions and the remaining residues in additionally allowed regions. The overall fold is similar to that of the previously reported structures (Sekar, Sekharudu *et al.*, 1998; Sekar & Sundaralingam, 1999; Steiner *et al.*, 2001). In the present anisotropic model, the side chains of 25 residues have been modelled in two discrete alternate conformations and the atoms are clearly visible in the electron-density map contoured at the 1.2σ level.

3.2. Surface loop

The refined model shows well defined electron density for all the residues in the surface loop in the region of positions 60–70 (Fig. 1). Superposition of the backbone atoms of the surface-loop residues with those of the monoclinic triple mutant (K56,120,121M; Rajakannan *et al.*, 2002) shows a root-mean-square (r.m.s.) deviation of 0.31 Å (Fig. 2*a*). However, the deviation of the corresponding residues is 2.53 Å (PDB code 1une) and 2.55 Å (PDB code 1g4i), respectively (Fig. 2*b*), when superimposed with corresponding residues in the orthorhombic forms (Sekar & Sundaralingam, 1999; Steiner *et al.*, 2001).

3.3. Second calcium ion

As observed earlier in the triple mutant K56,120,121M (Rajakannan *et al.*, 2002), the present atomic resolution model also features a second calcium ion, which is coordinated by six ligand atoms (three from protein and three water molecules). The protein-ligand atoms are the side-chain atom $O^{\delta1}$ of Asn71, the backbone carbonyl O atom of Asn72 and the carboxylate atom $O^{\varepsilon2}$ of Glu92 and the ligand distances are 2.29, 2.37 and 2.35 Å, respectively. The three water-ligand distances are 2.31, 2.44 and 2.60 Å. One of the water molecules is modelled as having alternative positions, one of which is at a distance of 2.31 Å from the second calcium ion and the other at a distance of 2.37 Å. The occupancies are 0.7 and 0.3, respectively. The corresponding ligand distance in the earlier reported triple mutant (Rajakannan *et al.*, 2002) was 2.44 Å. All the three water O atoms liganded to the second calcium ion are involved in indirect hydrogen bonding (Figs. 2*a* and 2*b*) with the residues Ser60, Val65 and Asp66 in the surface loop through other water O atoms. To further substantiate

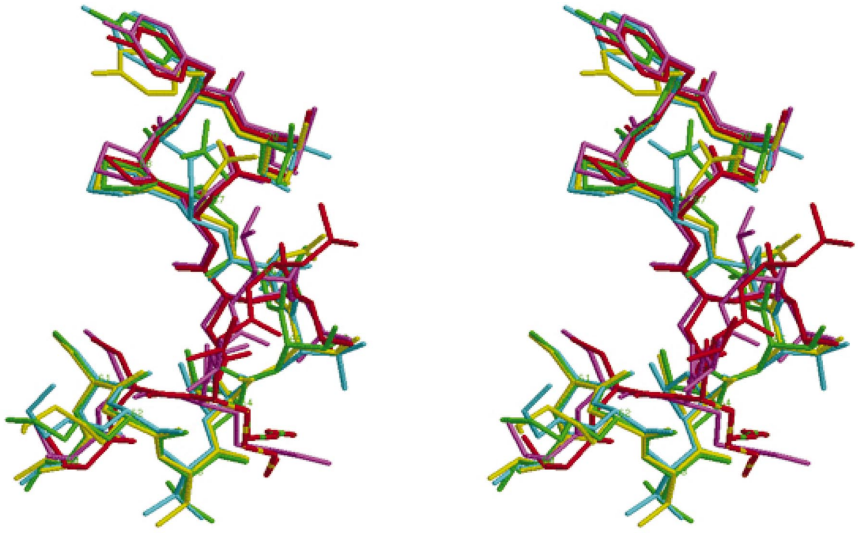

Figure 3
A stereoview showing the superposition of the surface-loop residues observed in the inhibitor-bound PLA_2 structures (green, Sekar *et al.*, 2003; blue, Sekar, Eswaramoorthy *et al.*, 1997; yellow, Sekar, Kumar *et al.*, 1998) with the present structure (red) and the triple mutant K56,120,121M (violet; Rajakannan *et al.*, 2002). The former three structures are inhibitor-bound PLA_2 structures and the latter two are inhibitor-free PLA_2 structures with the second calcium ion.

this interaction, we compared the conformations of the surface loops in the inhibitor-bound PLA_2 structures (Sekar, Eswaramoorthy *et al.*, 1997; Sekar, Kumar *et al.*, 1998; Sekar *et al.*, 2003) with those in the structures where we have located the second calcium ion (the present model and the triple mutant K56,120,121M; Rajakannan *et al.*, 2002) and this comparison is shown in Fig. 3. It is clear that the conformation of the surface loop observed in PLA_2 structures where a second calcium ion is bound is different to that observed in structures of inhibitor-bound PLA_2 complexes. We propose that the hydrogen-bonding network induced by the second calcium ion is responsible for the alternate surface-loop conformation. While we suspect that crystal packing and the second calcium ion have roles to play, in the final analysis we are uncertain of what causes the ordering of the 60–70 loop. It would be interesting to see the conformation of the surface loop in a structure containing both inhibitor as well as the second calcium ion.

3.4. Chloride ion

A huge peak (>6σ) is observed in the present model and is assigned as a chloride ion. A literature survey showed that a chloride ion has been observed in the wild-type enzyme (Steiner *et al.*, 2001) in the same position that a strong peak is seen in the present study. The chloride ion makes close contacts with the side-chain N atom of Lys12 (3.15 Å), the main-chain N atom of Ile82 (3.15 Å) and Arg100 $N^{\delta 2}$ (3.44 Å).

3.5. Water molecules

A total of 243 water O atoms are modelled in the present model. Of these, 137 have unit occupancy and the remainder are partially occupied. The first hydration shell contains 201 water O atoms, while the second hydration shell contains 36. The remaining six water O atoms have no interactions with protein atoms, water O atoms in the hydration shells or ions.

3.6. MPD molecules

Six MPD molecules are observed in the present model, while five were found in the earlier atomic resolution study (Steiner *et al.*, 2001). One MPD molecule, located at the surface of the protein near the helix containing residues Glu17–Phe22, is common to both structures. The remaining five MPD molecules in the present structure are observed around the active-site calcium ion. Instead of a cluster of three MPD molecules (with partial occupancies) at the entrance of the hydrophobic channel leading to the active site (Steiner *et al.*, 2001), only one MPD molecule with full occupancy is observed in the present structure.

4. Conclusions

The present structure provides a second example of a second calcium ion bound near the N-terminus in these mutant PLA_2s. Additionally, efforts are under way to co-crystallize various potential inhibitors to the triple mutants (K53,56,121M and K56,120,121M) to determine whether the inhibitor binds to the second calcium ion and also to study the dynamics of the surface loop.

The authors gratefully acknowledge the use of interactive graphics-based molecular modelling at the Supercomputer Education and Research Centre and the Distributed Information Centre. DV thanks SAIC-Frederick Inc., Basic Research Program, BNL for the visiting scientist fellowship and also thanks the UGC for financial support. VR thanks the Council of Scientific and Industrial Research for a Senior Research Fellowship. The work in Dr Tsai's laboratory was supported by NIH grants GM 41788 and GM 57568.

References

Brünger, A. T. (1992). *Nature (London)*, **355**, 472–474.
Dennis, E. A. (1994). *J. Biol. Chem.* **269**, 13057–13060.
Dennis, E. A. (1997). *Trends Biochem. Sci.* **22**, 1–2.
Dijkstra, B. W., Drenth, J., Kalk, K. H. & Vandermaelen, P. J. (1978). *J. Mol. Biol.* **124**, 53–60.
Dijkstra, B. W., Kalk, K. H., Hol, W. G. J. & Drenth, J. (1981). *J. Mol. Biol.* **147**, 97–123.
Huang, B., Yu, B. Z., Rogers, J., Byeon, I. J., Sekar, K., Chen, X., Sundaralingam, M., Tsai, M.-D. & Jain, M. K. (1996). *Biochemistry*, **35**, 12164–12174.
Jones, T. A. (1985). *Methods Enzymol.* **115**, 157–171.
Laskowski, R. A., MacArthur, M. W., Moss, D. S. & Thornton, J. M. (1993). *J. Appl. Cryst.* **26**, 283–291.
Liu, X., Zhu, H., Huang, B., Rogers, J., Yu, B.-Z., Kumar, A., Jain, M. K., Sundaralingam, M. & Tsai, M.-D. (1995). *Biochemistry*, **34**, 7322–7334.
Murshudov, G. N., Vagin, A. A., Lebedev, A., Wilson, K. S. & Dodson, E. J. (1999). *Acta Cryst.* D**55**, 247–255.
Navaza, J. (1994). *Acta Cryst.* A**50**, 157–163.
Otwinowski, Z. & Minor, W. (1997). *Methods Enzymol.* **276**, 307–326.
Perrakis, A., Morris, R. J. & Lamzin, V. S. (1999). *Nature Struct. Biol.* **6**, 458–463.
Rajakannan, V., Yogavel, M., Poi, M.-J., Jeyaprakash, A. A., Jeyakanthan, J., Velmurugan, D., Tsai, M.-D. & Sekar, K. (2002). *J. Mol. Biol.* **324**, 755–762.
Scott, D. L., White, S. P., Otwinowski, Z., Yuan, W., Gelb, M. H. & Sigler, P. B. (1990). *Science*, **250**, 1541–1546.
Sekar, K., Biswas, R., Li, Y., Tsai, M.-D. & Sundaralingam, M. (1999). *Acta Cryst.* D**55**, 443–447.

Sekar, K., Eswaramoorthy, S., Jain, M. K. & Sundaralingam, M. (1997). *Biochemistry*, **36**, 14186–14191.
Sekar, K., Kumar, A., Liu, X., Tsai, M.-D., Gelb, M. H. & Sundaralingam, M. (1998). *Acta Cryst.* D**54**, 334–341.
Sekar, K., Rajakannan, V., Velmurugan, D., Yamane, T., Thirumurugan, R., Dauter, M. & Dauter, Z. (2004). *Acta Cryst.* D**60**, 1586–1590.
Sekar, K., Sekharudu, C., Tsai, M.-D. & Sundaralingam, M. (1998). *Acta Cryst.* D**54**, 342–346.
Sekar, K. & Sundaralingam, M. (1999). *Acta Cryst.* D**55**, 46–50.
Sekar, K., Vaijayanthi Mala, S., Yogavel, M., Velmurugan, D., Poi, M.-J., Vishwanath, B. S., Gowda, T. V., Jeyaprakash, A. A. & Tsai, M.-D. (2003). *J. Mol. Biol.* **333**, 367–376.
Sekar, K., Yu, B.-Z., Roger, J., Lutton, J., Liu, X., Chen, X., Tsai, M.-D., Jain, M. K. & Sundaralingam, M. (1997). *Biochemistry*, **36**, 3104–3114.
Sheldrick, G. M. & Schneider, T. R. (1997). *Methods Enzymol.* **277**, 319–343.
Steiner, R. A., Rozeboom, H. J., de Vries, A. A., Kalk, K. H., Murshudov, G. N., Wilson, K. S. & Dijkstra, B. W. (2001). *Acta Cryst.* D**57**, 516–526.
Thunnissen, M. M. G. M., Eiso, A. B., Kalk, K. H., Drenth, J., Dijkstra, B. W., Kuipers, O. P., Dijkman, R., de Haas, G. H. & Verheij, H. M. (1990). *Nature (London)*, **347**, 689–691.
Verheij, H. M., Volwerk, J. J., Jansen, E. H., Puyk, W. C., Dijkstra, B. W., Drenth, J. & de Haas, G. H. (1980). *Biochemistry*, **19**, 743–750.
Yu, B.-Z., Poi, M.-J., Ramagopal, U. A., Jain, R., Ramakumar, S., Berg, O. G., Tsai, M.-D., Sekar, K. & Jain, M. K. (2000). *Biochemistry*, **39**, 12312–12323.
Zhu, H., Dupureur, C. M., Zhang, X. & Tsai, M.-D. (1995). *Biochemistry*, **34**, 15307–15314.